CMS Conference Report

1 October 2006

Radiation-Hard Quartz Cerenkov Calorimeters

U. Akgun, Y. Onel (for CMS Collaboration)

Department of Physics and Astronomy, The University of Iowa, 203 Van Allen Hall, Iowa City IA, 52242, USA

Abstract

New generation hadron colliders are going to reach unprecedented energies and radiation levels. Quartz has been identified as a radiation-hard material that can be used for Cerenkov calorimeters of the future experiments. We report from the radiation hardness tests performed on quartz fibers, as well as the characteristics of the quartz fiber and plate Cerenkov calorimeters that have been built, designed, and proposed for the CMS experiment.

Presented in CALOR 2006, Chicago, June 2006

1 Introduction

The future colliders are going to reach unprecedented energies and the experiments will experience huge particle fluxes. This requires developing and using radiation hard detector system technologies. For the CMS Forward Calorimeter (HF) we have used quartz fibers as the active material, in light of a series of radiation-hardness tests performed on quartz fibers. We report results from these tests. In this paper we summarize the test beam results on Pre-Production Prototype (PPP-1) and HF, as well as the Geant4 simulations. The CMS detector has the CASTOR calorimeter behind HF to cover the forward region better. CASTOR has been designed to use Cerenkov light made in quartz plates. We review the design properties of CASTOR calorimeter. As a possible upgrade to the End-Cap Hadron calorimeter for the SuperLHC (SLHC) era, we have proposed to replace existing scintillators with radiation hard quartz plates. In the last section of this paper we give the preliminary results from $R\&D$ studies for maximizing the Cerenkov light collection efficiencies.

2 Radiation Damage Studies on Quartz Fibers

The simulations show that the CMS HF calorimeters are going to absorb, on average, 760 GeV energy per event. This is huge compared to only 100 GeV for the rest of the main detector. Moreover, this energy is not uniformly distributed, but has a pronounced maximum at the highest rapidities. At $\eta = 5$ and integrated luminosity of $5 \times 10^5 pb^{-1}$ (around 10 years of LHC operation), the HF will experience almost 1 GRad radiation [1]. The neutron rates ($E_n <= 14$ MeV) at the front of the detector will be in the order of $10^8 Hz/cm^2$. The charged hadron rates will also be extremely high, especially at the shower maximum of the HF where the rate will reach 10^{13} to $10^{16} Hz/cm^2$. This hostile environment presents a unique challenge in particle detection techniques.

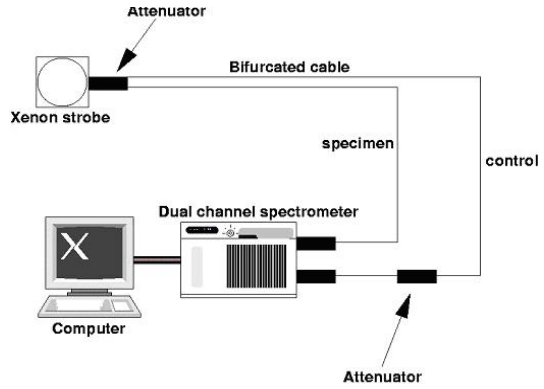

Figure 1: The experimental setup.

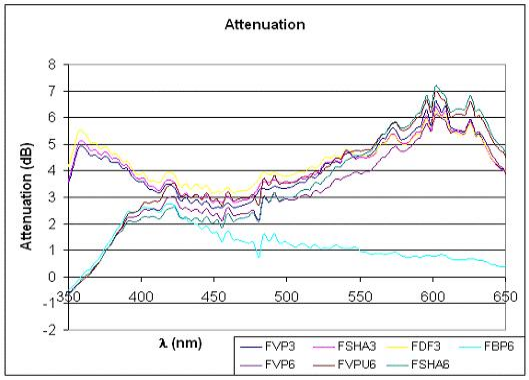

Figure 2: Attenuation for seven groups of fibers.

Initial radiation damage studies on quartz fibers were performed at two different facilities; a 10 kW experimental reactor, UTR-10 at ISU in Ames, Iowa, and the MGC-20E cyclotron at ATOMKI in Debrecen, Hungary. The details of these tests can be found elsewhere [2]. The initial tests showed some radiation recovery for most silica fibers. For some quartz fiber types < 10 MRad gamma irradiation seems to have generated a similar type of optical damage as neutron irradiation at fluence of $10^{15} n/cm^2$. After these initial tests we performed more radiation damage tests on nine different high OH- quartz fibers by irradiating them with 500 MeV electrons from the Linac Injector of LEP (LIL) at CERN. The transmission of Xe light was measured in-situ in the 350-800 nm range. The induced attenuation at 450 nm is found to be $1.52 \pm 0.15 dB/m$ for a 100 Mrad absorbed dose. We observed some darkening on the fibers, but the radiation did not change the tensile strength of the quartz fibers [3].

In 2004, quartz fibers were exposed to strong neutron and photon radiation and tested for optical degradation. The fibers were irradiated with pulses of high-energy neutrons produced by the Intense Pulsed Neutron Source (IPNS) at Argonne National Laboratory for a two-week period. Damage to the fibers was determined after $7.42 \times 10^{17} n/cm^2$ of fast neutrons, 17.6 Mrad of neutron and 73.5 Mrad of gamma radiation. The spectra of the irradiated fibers look similar to those from the non-irradiated fibers but were noticeably attenuated. The level of damage was wavelength specific (See Figure 1 and Figure 2). Recently, to complete our knowledge of radiation damage of the quartz fibers we initiated a high level of irradiation with 24 GeV protons at CERN. The quartz fibers with 0.6 mm core diameter were irradiated with $4.610^{16} protons/cm^2$ corresponding to a 1.2 Grad dose. The attenuation measurements were performed in-situ. We tested quartz fibers with quartz cladding (qq) and with plastic cladding (qp). The light

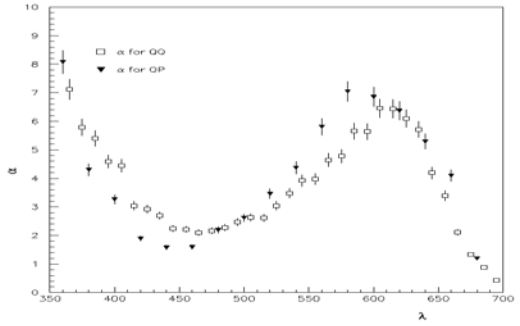

Figure 3: α parameters for qq and qp fibers versus wavelength, where α is the attenuation in dB/m at 100 Mrad.

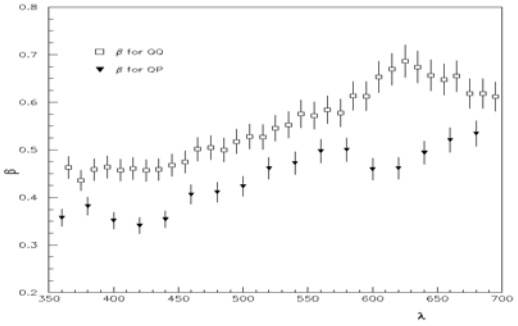

Figure 4: β parameters for qq and qp fibers versus wavelength.

attenuation in the fiber is defined as

$$A(\lambda, D) = \alpha(\lambda)[D/D_s]^{\beta(\lambda)}$$

Where α and β are parameters for qq and qp fibers that are determined by fitting the ratios as a function of wavelength and dose.

$$I(\lambda, D)/I(\lambda, 0) = e^{-[(L/4.343)\alpha(\lambda)(D/D_s)^{\beta(\lambda)}]}$$

Choosing a scale factor Ds = 100 Mrad, a is the attenuation at 100 Mrad, in dB/m, L being expressed in m (see Figure 3 and Figure 4). After 1.2 Grad of proton irradiation, the results are similar to the electron radiation tests [4]. Up to 0.8 Grad we do not observe a significant difference in attenuation versus dose between qq and qp fibers. Above 0.5 Grad there is no recovery of damage below 380 nm, and in the range of 580-650 nm quartz becomes opaque. We monitored the recovery over 4 months. The decrease of signal in fibers is very fast at the beginning: 30% loss after 20 Mrad at 455 nm.

3 Quartz Cerenkov Calorimeters of the CMS Experiment

This part of the paper will cover three different radiation-hard Cerenkov calorimeters for the CMS experiment (Figure 5); i) Pre-Production Prototype (PPP-1) of the Forward (HF) calorimeter, ii) The Forward (HF) calorimeter iii) The CASTOR calorimeter. The PPP-1, and HF use quartz fibers while CASTOR uses quartz plate as the active volume (Figure 6).

3.1 Pre-Production Prototype (PPP-1)

The PPP-I is an iron absorber matrix with embedded quartz fibers which serve as the active material. The iron matrix is composed of 2.5 mm thick iron layers with grooves every 2.5 mm. The embedded fibers run parallel to the beam and constitute the active component of the detector. The length of the absorber is 165 cm, 8.3 nuclear interaction length (λ_{int}), with a cross sectional area of $18cm \times 18cm$. A single quartz fiber is inserted In each groove. In PPP-I, there are three different lengths of fibers to achieve a longitudinal segmentation. They are called electromagnetic (EM), hadronic (HAD), and tail catcher (TC). Long fibers sample all shower components while the shorter fibers are biased to the hadron component as the hadronic showers tend to penetrate deeper. There are two EM fibers for each HAD and TC fiber. The PPP-I is divided into nine physical regions called towers, each with a 6 cm 6 cm cross sectional area. At the center of each tower, a radioactive wire source-tube groove exists for calibration [5].

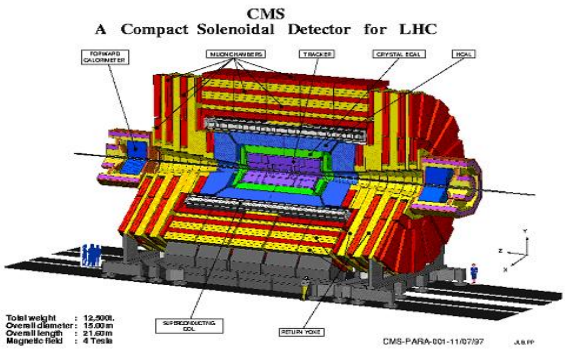

Figure 5: The major components of the central part of the CMS detector.

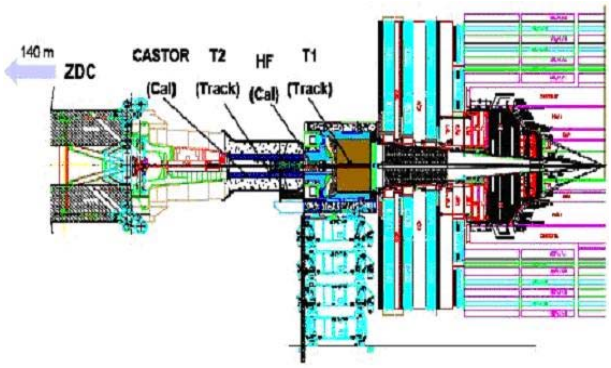

Figure 6: The major components of the forward region of the CMS detector.

At the test beam the detector was placed on a platform that could move in three dimensions with respect to the H4 beam line at CERN. One of the factors that affect the calorimeters response is the non-uniformities in its structure. In PPP-I, this non-uniformity is the fiber spacing. In order to study the spatial uniformity of the PPP-I, a 120 GeV electron beam was moved with 1.0 cm steps across the face of the detector. The energy resolution of a calorimeter, in general, can be parametrized as

$$(\sigma/E)^2 = (a/\sqrt{E})^2 + (b/E)^2 + c^2$$

The first term is the sampling term and characterizes the statistical fluctuations in the signal generating processes. The second term corresponds to noise and includes the energy equivalent of electronic noise as well as pileup. The third term is the constant term and is related to the imperfections of the calorimetry, signal generation and collection non-uniformity, calibration errors and fluctuations in the energy leakage from the calorimeter. In quartz fiber calorimeters the electromagnetic energy resolution is completely dominated by photoelectron fluctuations, therefore we drop the noise term for electromagnetic resolution definition (See Figure 7). The electromagnetic energy resolution was measured to be

$$(\sigma/E)^2 = (197\%/\sqrt{E})^2 + (8\%)^2$$

Where, E has units of GeV. The hadronic energy resolution was determined to be 18% at 1 TeV (Figure 8).

3.2 The Forward (HF) Calorimeters

The HF calorimeters consist of two modules, located symmetrically at about 11 m from either side of interaction point. They cover the pseudorapidity range 3-5. The length along the beam is 1.65 m or 10 λ_{int}. Each calorimeter consists of a large steel block that serves as the absorber. Embedded quartz fibers in the steel absorber run parallel to the beam and constitute the active component of the detector. In order to optimize energy resolution for E and E_T flows and forward jets, the calorimeter is effectively segmented longitudinally by using two different fiber lengths.

In this report we will summarize the results from tests performed on HF modules at the H2 test beam line at CERN, in 2004. And, the Geant4 simulation efforts to verify the test beam. The HF wedges were individually placed on a remotely controlled table that could move horizontally and vertically with respect to the beam with better than 1 mm precision. The angular positioning of the detector on the vertical plane with respect to the beam line was also remotely controlled and varied from 0^o to 6^o to mimic the particle path in the CMS experiment. The purity of the beam depended on energy; in particular, high energy electron beams were contaminated with pions and muons [6]. The simulations of the test beam, the physics of the electromagnetic and hadronic processes, are implemented by using GEANT4 physics applications. Although electromagnetic physics used in the simulation is standard GEANT4 electromagnetic physics, four different physics lists are used for the hadronic physics, LHEP, QGSP, QGSC, and FTFP [7]. Table 1 and Table 2 summarize the comparison of different Geant4 simulations with

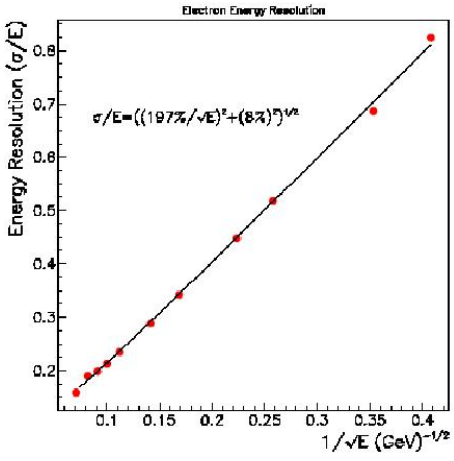

Figure 7: The electromagnetic energy resolution of PPP-1 as a function of $1/\sqrt{E}$.

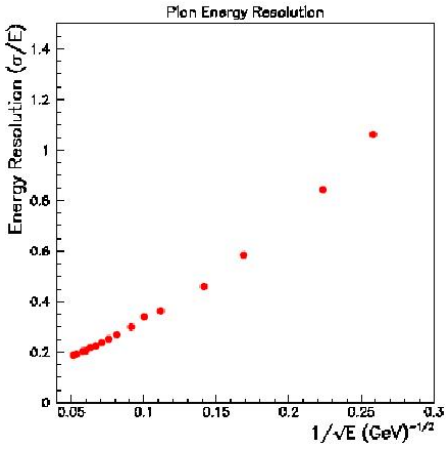

Figure 8: The hadronic energy resolution of PPP-1 as a function of $1/\sqrt{E}$.

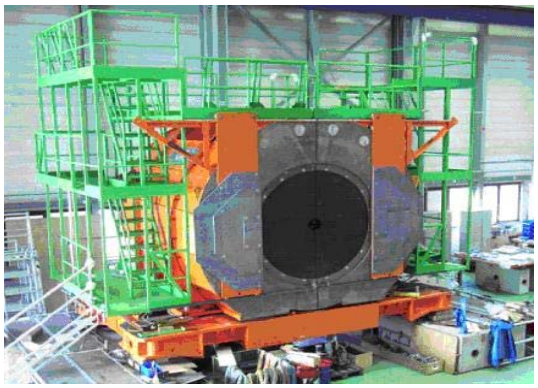

Figure 9: One of the completed HF calorimeters in CERN.

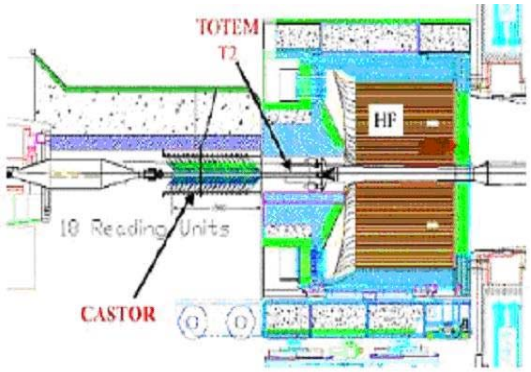

Figure 10: The Forward region detectors.

the test beam. The test beam results showed that for the electromagnetic energy resolution, the stochastic term a is 198% and the constant term c is 9%. The hadronic energy resolution is largely determined by the fluctuations in the neutral pion production in showers, with $a = 280\%$ and $c = 11\%$.

Table 1: Test beam electromagnetic energy resolution and Geant4 results.

Data	30 GeV	50 GeV	100 GeV	150 GeV
TB04	0.396 ± 0.028	0.315 ± 0.022	0.231 ± 0.016	0.204 ± 0.014
LHEP	0.421 ± 0.001	0.329 ± 0.001	0.239 ± 0.001	0.201 ± 0.001
QGSP	0.420 ± 0.001	0.328 ± 0.001	0.240 ± 0.001	0.201 ± 0.001
QGSC	0.421 ± 0.001	0.328 ± 0.001	0.239 ± 0.001	0.203 ± 0.001
FTFP	0.422 ± 0.001	0.328 ± 0.001	0.238 ± 0.001	0.203 ± 0.001

Table 2: Test beam hadronic energy resolution and Geant4 results.

Data	30 GeV	50 GeV	100 GeV	150 GeV
TB04	0.514 0.036	0.407 0.029	0.309 0.022	0.267 0.019
LHEP	0.495 ± 0.001	0.380 ± 0.001	0.280 ± 0.001	0.241 ± 0.001
QGSP	0.467 ± 0.001	0.368 ± 0.001	0.275 ± 0.001	0.234 ± 0.001
QGSC	0.477 ± 0.001	0.373 ± 0.001	0.276 ± 0.001	0.236 ± 0.001
FTFP	0.466 ± 0.001	0.372 ± 0.001	0.274 ± 0.001	0.232 ± 0.001

3.3 CASTOR Calorimeter

CASTOR [8] is a calorimeter that will measure the energy of particles emitted at very small angles, covering the polar angles from 0.1^o to 0.7^o with respect to the beam direction. The detector is an octagonal cylinder, approximately 1.5 m long with an outer diameter of 36 cm and an inner diameter of 3.8 cm (to contain the beam pipe). It is subdivided into 16 sections in azimuth and 18 sections in depth. This fine segmentation allows it to image the 3 dimensional texture of energy deposition for different particles. Because the energy of the incoming particles is very high, the CASTOR spectrometer has to be very dense, which is achieved by using tungsten plates. For sensitivity to the angle of the incoming particles it is desirable to measure only the very fast positrons and electrons produced at small angles with respect to the initial direction. This is done by using the Cerenkov effect, which results in emitted light created in an approximate electromagnetic equivalent to the shock front that causes sonic booms. In its proposed location, the detector is expected to experience radiation exposure in the range of 10-100 MGy. The quartz is arranged in thin plates, tilted at 45^o in order to efficiently capture the Cerenkov light. In order to increase the amount of light collected, many layers of tungsten and quartz are stacked together. The light from seven quartz plates is collected by an air filled light guide, covering 22.5o in azimuthal angle (see Figure 11).

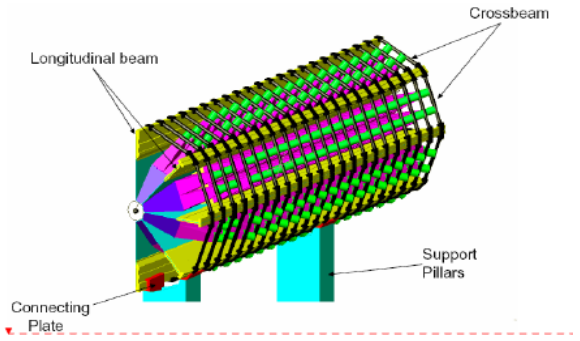

Figure 11: The design of CASTOR.

The electromagnetic particles, photons and electrons, penetrate less deeply into the detector than the hadronic particles, such as pions and protons. Therefore, the first 11.5 cm of the detector is segmented slightly differently with tungsten and quartz thicknesses of 3.0 and 1.5 mm, respectively, compared to 5.0 and 2.0 mm, in the remaining 1.25 m hadronic section of the device. With this design of quartz detectors, the diameter of the showers of electrons and positrons produced by hadrons is of the order of 1 cm for tungsten, compared to values orders of magnitude larger in other calorimeters. CASTOR will provide a very fast, high resolution measure of the azimuthal distribution of energy in a region very close to the beam direction. The longitudinal segmentation will allow this energy to be differentiated into that carried by hadronic and electromagnetic particles and to allow study of exotic objects that have been predicted to occur in this angular range [9]. In events with smaller occupancy, the energy of individual particles, as well as their hadronic or electromagnetic nature, can be determined with high accuracy.

4 CMS HCAL Detector Upgrade Studies For SLHC

The Large Hadron Collider (LHC) is designed to provide, 14 TeV center of mass energy with proton-proton collisions every 25 ns. After a few years of run, the conditions of LHC will be upgraded to operate at 10 times higher luminosity ($L = 10^{35} cm^{-2} s^{-1}$) allowing new physics discoveries. This period is called SLHC. In the current design, Hadronic EndCap (HE) calorimeters of the CMS experiment use Kuraray SCSN81 scintillator tiles, and Kuraray Y-11 double clad wavelength shifting fiber. These materials have been shown to be moderately radiation hard up to 2.5 MRad [1]. The scintillation photons are collected by wavelength shifting fibers which have the geometry shown in the first picture at Figure 12. Under the SLHC conditions the lifetime radiation dose at the HE will increase from 2.5 Mrad to 25 Mrad. The scintillator tiles used in the current design of HE will lose their efficiency due to high radiation. As a solution to the radiation damage problem with SLHC conditions, we propose to replace the scintillators with quartz plates. They will not be affected by the high radiation, but with quartz plates, the light comes from Cerenkov radiation which produces 100 times less light than scintillation. Our aim is to find an efficient way to collect light from quartz plates. At the University of Iowa and Fermilab, we tested and simulated different sizes of quartz plates with different fiber geometries embedded in them to obtain maximum light. After the test beams and simulations of different fiber geometries for their light collection efficiencies and uniformities we have constructed a quartz plate calorimeter prototype. The Geant4 simulations for the calorimeter prototype are still undergoing. We have test beams scheduled at Fermilab and CERN for the fall of 2006.

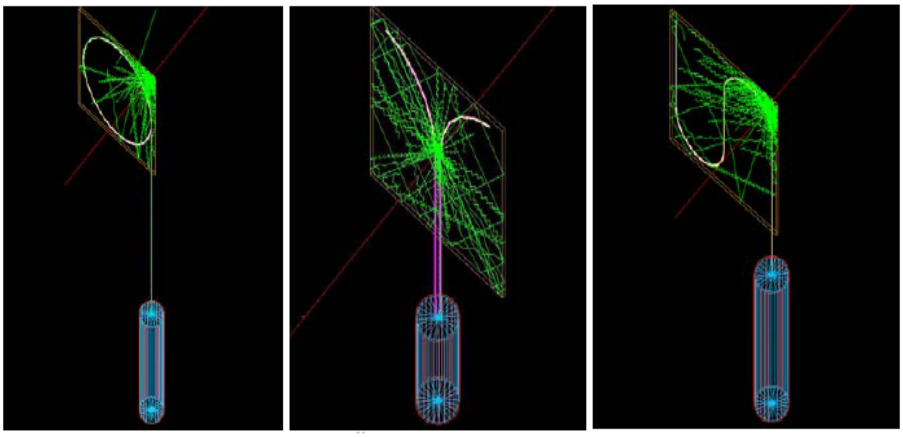

Figure 12: Geant4 simulations of the Cerenkov light collection in quartz plates with different fiber geometries.

5 Acknowledgements

We would like to thank D. Green, J. Freeman, and A. Skuja of HCAL management, P. Bruecken, K. Cankocak, J.P. Merlo, T. Yetkin, IowaTurkish Universities Raddam Group. E. Norbeck, A.D. Panagiotou of the CASTOR group. This research is funded by DOE (DE-FG02-91ER40644), Iowa-Fermilab MOU for CMS construction and $M\&O$ projects, and The University of Iowa office of VP of Research and Graduate College.

References

[1] *The Hadron Calorimeter Project Technical Design Report*, **CERN/LHCC 97-31**, CMS TDR 2, 20 June 1997.

[2] **A.S. Ayan**, *The CMS Forward Calorimeter Prototype Design Studies and Oc0 Search at E781 Experiment at Fermilab*, Ph.D. Thesis, The University of Iowa, 2004.

[3] **I. Dumanoglu et al.**, *Radiation-hardness studies of high OH- content quartz fibres irradiated with 500 MeV electrons*, Nucl. Instrum. Meth. A 490, 2002, 444-455.

[4] **J.P. Merlo and K. Cankocak**, *Radiation-hardness studies of high OH- content quartz fibers irradiated with 24 GeV protons*, 2006, CMS CR 2006/005.

[5] **A.S. Ayan et al.**, *Energy resolution and the linearity of the CMS forward quartz fibre calorimeter*, J. Phys. G: Nucl. Part. Phys., 30, (2004), N33-44.

[6] **G. Baiatian et al.**, *Design, Performance, and Calibration of the CMS Forward Calorimeter Wedges*, CSM NOTE 2006/044.

[7] **T. Yetkin**, *Search for SUSY in Missing Transverse Energy Plus Multijet Topologies at vs = 14 TeV and Geant4 Simulation of the CMS Hadronic Forward Calorimeter in the 2004 Test Beam*, Ph.D. Thesis, Cukurova University, 2006.

[8] **CASTOR: Centauro And Strange Object Research, http://cmsdoc.cern.ch/castor**

[9] **E. Gladysz-Dziadus**, *CASTOR: Centauro and Strange Object Research Exotic Aspects of Forward Physics at the LHC*, Act. Phys. Pol. B, 37, 2006, 153-160.